CrossMark

Molecular imprinted polymer-coated optical fiber sensor for the identification of low molecular weight molecules

Sandrine Lépinay [a,b,*], Anatoli Ianoul [b], Jacques Albert [a]

[a] Department of Electronic, Carleton University, 1125 Colonel By Drive, Ottawa, ON, Canada K1S 5B6
[b] Department of Chemistry, Carleton University, 1125 Colonel By Drive, Ottawa, ON, Canada K1S 5B6

ABSTRACT

A biomimetic optical probe for detecting low molecular weight molecules (maltol, 3-hydroxy-2-methyl-4H-pyran-4-one, molecular weight of 126.11 g/mol), was designed, fabricated, and characterized. The sensor couples a molecular imprinted polymer (MIP) and the Bragg grating refractometry technology into an optical fiber. The probe is fabricated first by inscribing tilted grating planes in the core of the fiber, and then by photopolymerization to immobilize a maltol imprinted MIP on the fiber cladding surface over the Bragg grating. The sensor response to the presence of maltol in different media is obtained by spectral interrogation of the fiber transmission signal. The results showed that the limit of detection of the sensor reached 1 ng/mL in pure water with a sensitivity of 6.3×10^8 pm/M. The selectivity of the sensor against other compounds and its reusability were also studied experimentally. Finally, the unambiguous detection of concentrations as little as 10 nM of maltol in complex media (real food samples) by the MIP-coated tilted fiber Bragg grating sensor was demonstrated.

© 2014 Elsevier B.V. All rights reserved.

1. Introduction

The rapid and sensitive detection of analytes at low concentrations has become important in many fields such as medicine, environmental monitoring and food safety. Many devices have been developed to detect binding events but the current challenge is to design simple, inexpensive, accurate, sensitive and reliable sensors [1–3]. In this context, sensing layers are crucially needed. Biological materials are often used to detect binding events, for instance enzyme-linked immunosorbent assay (ELISA) and antibodies. But over the last few decades, molecular imprinting has also been extensively developed and used for detecting molecular species [4–7]. Indeed, the molecular imprinting technique is a well-established approach to develop biomimetic materials able to recognize specifically an analyte from closely related compound mixtures [8]. For the preparation of a film of molecular imprinted polymer (MIP) on a surface, several techniques can be used. Among these, the "grafting from" technique allows a robust bond between the transducer surface and the sensing layer. It can produce films with nanometer thicknesses and it is easy to carry out. Here a common functional monomer was used, acrylic acid, for its ability to provide hydrogen bonds within the template. The complex

acrylic acid-template was then photopolymerized with the cross-linking monomer, ethylene glycol dimethacrylate, in presence of dichloromethane. Subsequently, the template was extracted with a strong acid solution. The molecular imprinted surface results in tailor-made receptor cavities complementary in size, shape and chemical functionality to those of the template molecule. As a result, the template molecule can easily rebind with the cavities left in the matrix polymer of the MIP [9]. The use of ethylene glycol dimethacrylate as a crosslinker is required to solidify the polymer network in three dimensions and to maintain the structural integrity of the binding sites. Hence, the detection is based on a "key and lock" model. Because of their high stability, strong reusability, low cost and easy synthesis, MIPs present a number of advantages for sensing in comparison to bioreceptors [10–12].

Another aspect to be considered when developing a sensor of real practical utility is its size. In this regard, optical fiber sensors are an appealing solution [3,5,13,14]. Indeed, optical fibers are tiny, flexible, compact and cost-effective which explain their increasing presence as sensor platforms. In fiber sensors, light guided in the core has to escape into the cladding to allow an interaction with the external medium and perform measurements. Several configurations can be implemented in fibers to allow this interaction, for instance, etching [15], side polishing [16], or tapering the fiber [17]. The excitation of cladding modes can also be carried out with the tilted fiber Bragg gratings (TFBG) [18]. These devices are made from a standard telecommunication single mode fiber modified by internal grating

* Corresponding author at: Department of Electronic, Carleton University, 1125 Colonel By Drive, Ottawa, ON, Canada K1S 5B6. Tel.: +1 613 520 2600x1636.
E-mail address: slepinay@connect.carleton.ca (S. Lépinay).

planes oriented a few degrees away from the perpendicular to the fiber axis. The grating tilt allows a strong coupling between the core guided light and a large number of cladding modes. A TFBG sensor can be used for sensing in media with refractive indices ranging from 1.25 to 1.4. The transduction method of TFBGs is based on measurable refractive index changes at the interface between the optical device and the surrounding medium, deriving from the interaction of an analyte with a receptor attached to the cladding surface. MIPs have been widely used for specific sensors based on different transduction methods, such as electrochemistry, QCM sensors or Raman spectroscopy [19–22]. However, only a few sensors have been found in the literature in which MIPs are used with optical fibers [17,47]. Otherwise most of the fiber-based biochemical sensors presented so far used metal coated optical fibers combined with a conventional surface plasmon effect but recently a higher figure of merit configuration that uses plasmon-modified narrowband spectral resonances from metal-coated TFBGs was demonstrated [23–28]. In the latter configuration, when the plasmon resonance condition is reached, a transfer of energy from the incident core guided light to a surface plasmon wave occurs and the transmissivity of the TFBG changes significantly [26]. It was also determined however, that even in the absence of plasmonic enhancement, the narrowband resonance condition for the coupling of core-guided light to cladding-guided light is also highly sensitive to the refractive index of the dielectric medium adjacent to the fiber cladding surface and hence can be used to detect minute changes, such as those occurring when a molecule fills its niche inside a MIP coating on the fiber [18]. The measurement of the spectral transmission of the coated TFBG thus reveals the capture of molecules by the MIP layer. Since the spectral resonances of TFBGs are very narrow ($\sim$ 100 pm), it is possible to follow wavelength shifts in the range of a few picometers, thus making the TFBG platform very sensitive and accurate. Previously determined limits of detection (LOD) using TFBG-SPR were determined to be 22.6 nM for the binding of aptamers [27], 2 pM for avidin recognition [28] and 8 pM using LSPR for the detection of biotin [29]. Only one paper reported biological sensing using the bare silica surface of TFBG (i.e. without SPR) and the authors were able to detect a 86 µg/L concentration of anti-BSA [30].

In the present paper, we have carried out the fabrication and characterization of a fiber optic sensor for the detection of a low molecular weight molecule, maltol (3-hydroxy-2-methyl-4H-pyran-4-one, molecular weight MW=126.11 g/mol) which is used as a model molecule. The tilted fiber Bragg grating is used as the optical transducer, while the MIP technique is used to functionalize the transducer for the molecule of interest.

Maltol is an aroma enhancer additive known as INS 636 in the International Numbering System of the codex alimentarius. This aroma is somewhat controversial because it is believed that it can increase the adsorption of some metals such as Fe^{3+}, Ga^{3+}, and Al^{3+} in the human body, with potential harmful consequences [31–34]. Several countries have forbidden its use in children food and it is not allowed at all in the European Union [35,36]. So, the analysis of maltol is a potentially important test case in food quality control. While, ion chromatography can be used to determine the quantity of maltol in real food after several extraction cycles [37], this method is cumbersome, expensive and time consuming. Hence, the optical sensor proposed here can be a new practical alternative for the detection of maltol and by extension of other substances with similar molecular weight.

2. Materials and methods

2.1. Chemicals

Maltol, 3-(trimethoxysilyl) propyl methacrylate (γMAPS), acetic acid, methanol, dichloromethane and ethyl maltol, 2,2′-azobisisobutyronitrile (AIBN), acrylic acid (AA) and ethylene glycol dimethacrylate (EDMA) were purchased from Sigma-Aldrich. Hydrochloric acid (HCl), sodium hydroxide (NaOH) and dichloromethane were purchased from VWR. The chemicals were used directly except for AIBN, acrylic acid and EDMA which were purified before use. A commercial fruit-flavoured jelly powder was used as a typical complex food sample test solution. Doubly deionized water was obtained from a Milli-Q water purification system, resistivity $\geq$ 18.2 MΩ cm (Thermo Fisher Scientific Inc.) and was used in all assays and solutions.

2.2. Optical sensor system

Figs. 1A and B shows the tilted fiber Bragg grating (TFBG) sensor system. A standard single-mode optical fiber (Corning SMF-28) was used as an optical sensor [38]. The Bragg grating with a 10° tilt was inscribed by an intense ultraviolet laser light pattern (generated by a diffractive phase mask) in the fiber core. These grating planes with this specific angle allow core-guided light to escape into the cladding which is in contact with the outer medium. At this grating tilt angle, the optical sensor can operate in aqueous solutions with refractive indices between 1.31 and 1.34 [39]. To provide a convenient and easy way to use the sensor, a thin gold mirror was formed on the downstream end of the Bragg grating by the electroless deposition [40]. In this configuration, the fiber end that contains the grating is simply dipped directly into the samples to be measured. The gold mirror redirects the light transmitted through the fiber core back towards the detector where its spectrum is measured.

A typical transmission spectrum obtained with the TFBG sensor submerged in water is presented in Fig. 1C. The wavelength denoted by the arrow represents the cladding resonance known to be the most sensitive to coupling interactions, i.e. the last mode guided by the cladding (so called "cut-off" mode) [14]. This mode is the one with an evanescent field that has the maximum penetration in the outer medium while still being confined by the cladding, and hence maximum sensitivity to changes occurring on top of the cladding. The analysis presented in this paper is based on tracking the changes to the cut-off wavelength of this mode, located approximately at 1538 nm. The analysis of the transmission signal changes was carried out by tracking the intensity of this transmission loss peak as well as the shifting of its wavelength away from its original position. This method can be accurately applied when the change of refractive index to be measured is relatively small between samples.

2.3. Chemical preparation of the TFBG sensor

The fabrication of the TFBG sensor required several steps as shown in Fig. 2. The bare fiber surface had to be prepared to allow a covalent attachment of the MIP film. The TFBG was cleaned by immersion in 0.1% HCl solution for 20 min, and then with NaOH (1 M) for 30 min and finally followed by several rinses in water. A vinylization of the TFBG surface is needed to introduce vinyl groups (C=C) on the surface of the TFBG from the OH groups at the silica surface [41]. Typically, γMAPS (2%) in toluene was left in contact with the fiber for 2 h. The fiber was then washed and rinsed to remove the excess of γMAPS. After rinsing, the optical fiber was dried in an oven at 60 °C for two hours.

For the polymerization, a mixture containing 1.9 mL EDMA, 90 µL acrylic acid, 1% AIBN, and 1 mM maltol in 5 mL of dichloromethane was prepared and sonicated at 0 °C for 10 min. Afterward the TFBG modified with γMAPS was immersed in a narrow test tube that was hermetically sealed and the solution was purged with nitrogen. Polymerization was carried out under UV-light (365 nm) irradiation for 1200 s. As a reference, a non imprinted polymer coated TFBG sensor (NIP) was also prepared in a similar manner as with MIP but without the maltol template molecules.
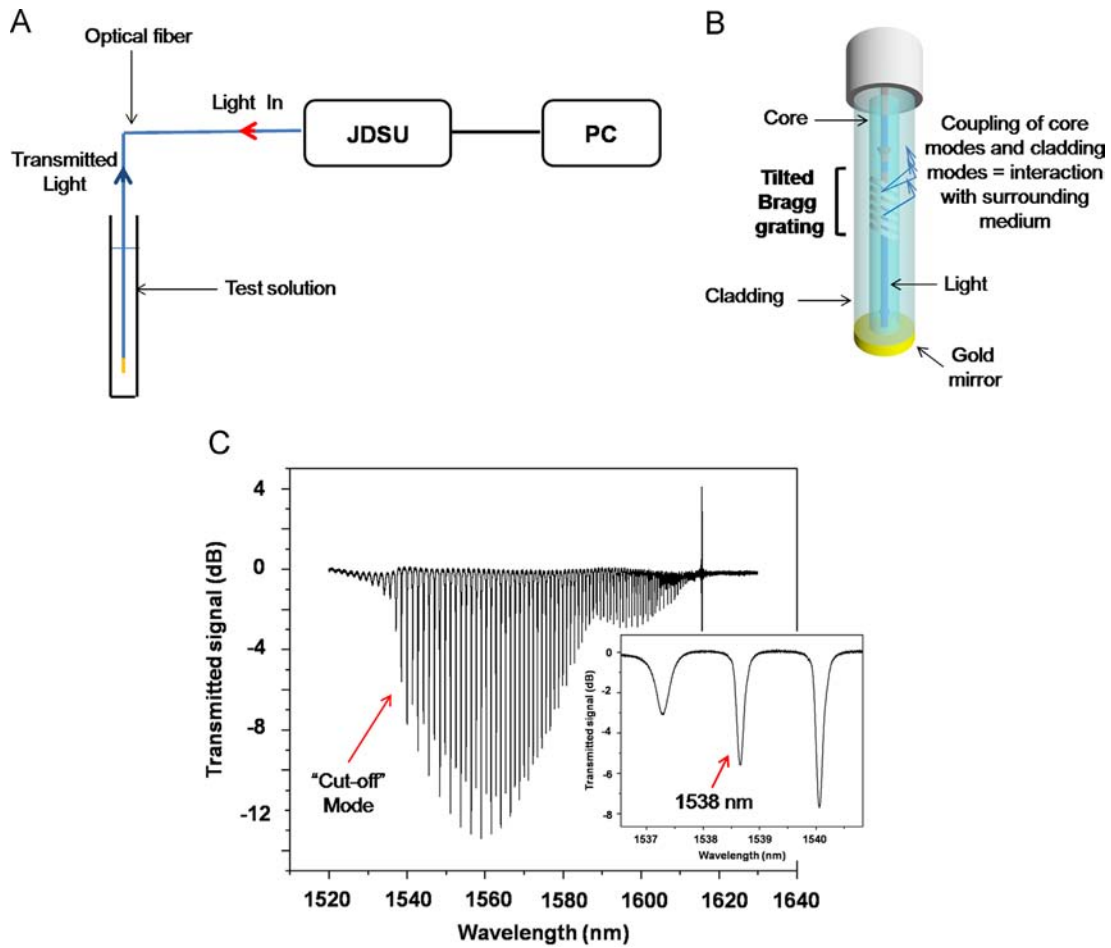
Fig. 1. (A) Experimental setup, (B) TFBG principle, and (C) typical spectrum obtained in aqueous solutions, the insert is a focus on the "cut-off" mode (1538 nm).
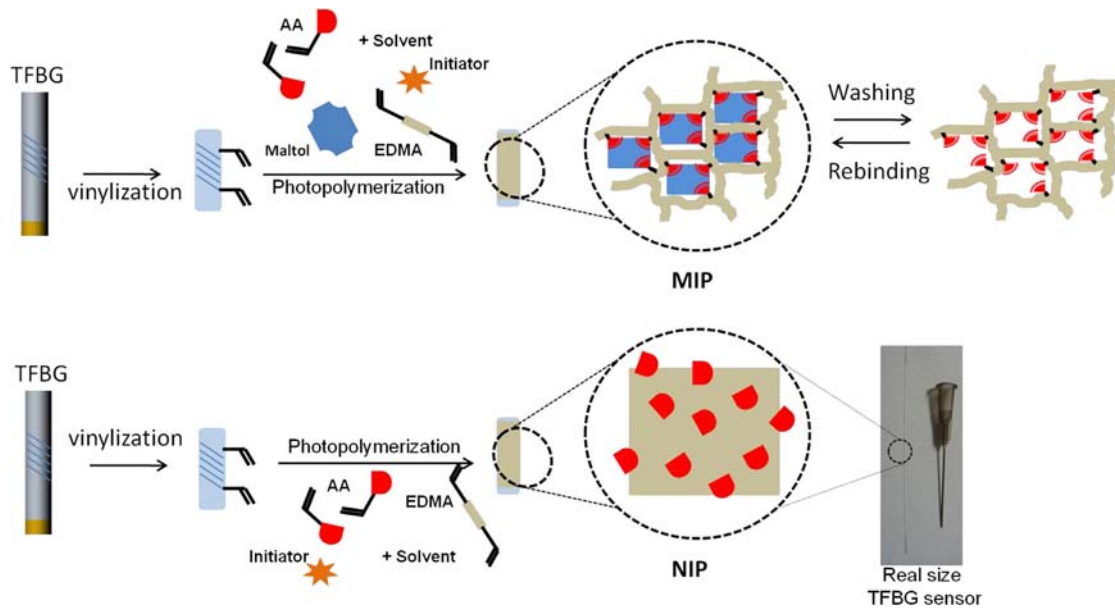

Fig. 2. Schematic representation of the molecular imprinting technique applied for the TFBG nanosensor. The picture shows the real size of the sensor compared with a 0.45 mm needle.

2.4. Monitoring of imprinted TFBG sensor response

The interactions between MIP and the corresponding target molecule are usually studied by batch rebinding experiments. This technique is cumbersome and the polymer in the form of small particles is not uniform [42–44]. For these reasons, in this study, the characterization of the interactions between maltol and the corresponding MIP were carried out by an optical method. A maltol-imprinted TFBG nanosensor was used for detection of maltol molecules dissolved in Milli-Q water. The measurements were performed by immersing the

optical fiber, either with or without MIP, in aqueous solutions of the target molecule (maltol) with an incubation time of 10 min. The transmission spectra were then recorded after 10 min of rinsing in water. The experimental spectra, normalized to the reference spectrum corresponding to pure water, were evaluated and the shifts obtained for the 1538 nm wavelength resonance were reported.

2.5. Selectivity of TFBG MIP sensor

The selectivity of the sensor for maltol was evaluated by comparing results obtained by using identical concentrations of ethyl maltol which is similar in chemical structure with maltol (Fig. 3). As before, the maltol–MIP–TFBG probe was immersed in ethyl maltol solutions for 10 min then rinsed with water for 10 more minutes before measuring the transmitted signal.

3. Results and discussion

3.1. Surface characterization of MIP and NIP by AFM

Fig. 4 shows the surface topography of the MIP and NIP after washing with methanol/acetic acid. The AFM images reveal a good coverage of the sensors surface. In the images scanned over an area of $10 \times 10 \ \mu m^2$, a difference in the surface roughness can be seen and expressed in terms of a root mean square value: after washing, the MIP has a rougher surface with a root mean square value of 3.7 nm while the NIP surface is characterized by a 2.4 nm root mean square value.
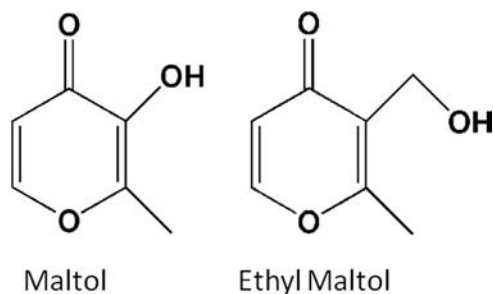

Fig. 3. Chemical structures of the template molecule (maltol) and the comparable but non-identical molecule (ethyl maltol) used in this study.

3.2. Measurement of binding interaction of MIP TFBG sensor

Because of its carboxylic group, acrylic acid is an amphoteric molecule and has the property to provide either hydrogen bonds or electrostatic bonds. From the maltol chemical structure, only hydrogen bonds allow an interaction between maltol and acrylic acid. The acidity constant of acrylic acid is 4.35. Above this value, the acid group is not protonated and become a carboxylate group (COO^-) and electrostatic bonds are preferred. Below 4.35, the carboxylic group is protonated (COOH) and the hydrogen bonds can be formed with an electronegative atom composing the maltol molecule. The first study was realized at neutral pH (experiment not shown). The maximum shift observed for the highest maltol concentration is less than 30 pm. The same experiment was then realized with an acidic pH, and the shift obtained is close to 45 pm. Following these experiments, all further tests were made with acid pH solutions.

To characterize the maltol–MIP nanosensor, different concentrations of maltol samples were used and their transmitted spectra were recorded. The binding of the maltol to the maltol–MIP on a TFBG induces a wavelength shift, $\Delta\lambda$. Fig. 5 depicts the signal shift ($\Delta\lambda$), versus maltol concentration. $\Delta\lambda$ is defined as $\lambda - \lambda_0$, where λ_0 was the exact position of the 1538 nm wavelength resonance measured in pure water and without the templates from the polymer matrix and λ was the position of the same resonance after immersion of the sensor into a maltol solution, incubation and rinsing. Solid squares, circles and triangles represent the wavelength shifts obtained from the transmitted spectra. The error bars were calculated from the spread between five measurements. The resonance shifts for the MIP–maltol optical nanosensor (data represented by the circles) in contact with maltol samples increased rapidly at lower maltol concentrations and then reached a plateau at high concentrations. This indicates signal saturation and a complete occupation of the available binding sites. The red-shift observed was 42.3 pm. Moreover, when the maltol–MIP nanosensor was immersed in the solution with the competing molecule, ethyl maltol (triangles) at the same concentrations, the total red-shift was only 9 pm. A similar behavior was obtained when the NIP sensor was put in contact with maltol molecules (squares): the wavelength shifts stayed under 5 pm. From these results it is concluded that the maltol–MIP sensor is $\sim 4 \times$ more selective for maltol than for ethyl maltol. This provides a good support for the selectivity of the molecular imprinted polymer (maltol–MIP) and the recognition capacities of the templates molecules.
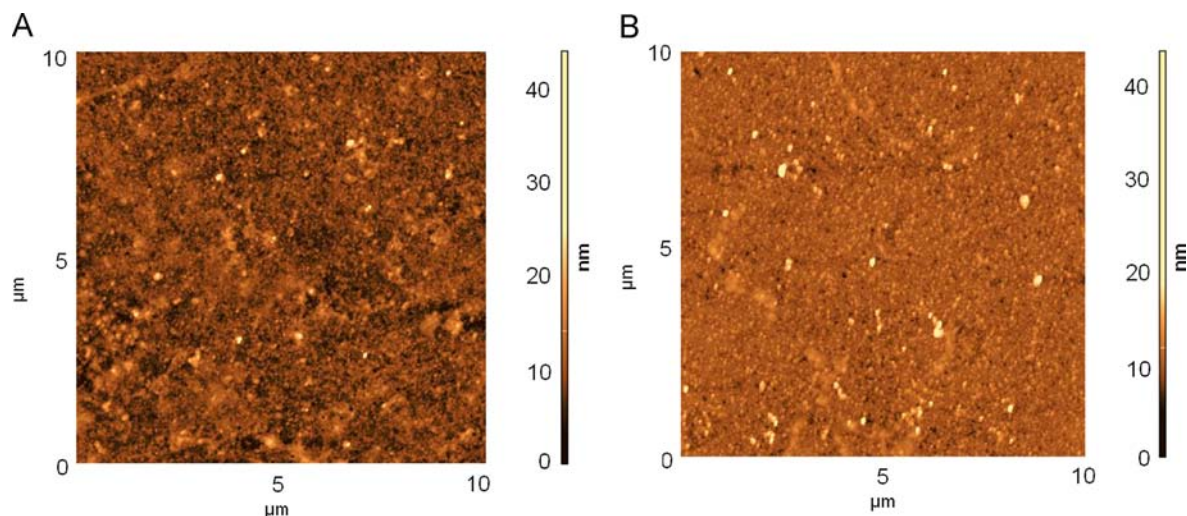

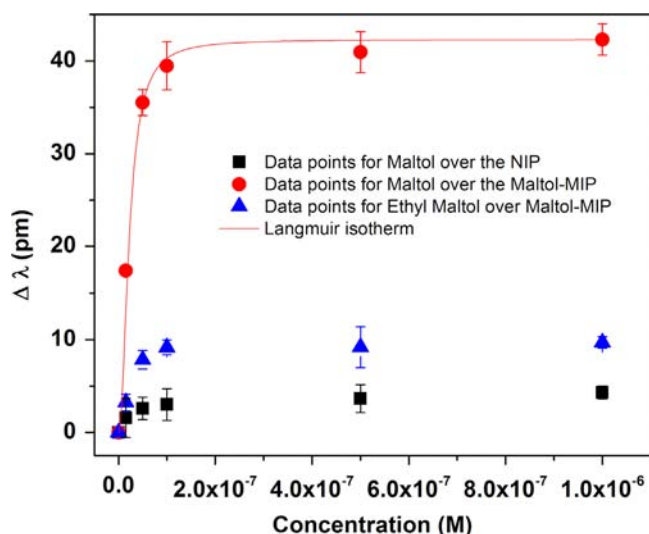**Fig. 4.** AFM micrographs of (A) MIP and (B) NIP sensors after washing.

Fig. 5. Variation of the shift in wavelength of the resonance with the concentration of the maltol and ethyl maltol samples over maltol–MIP–TFBG and NIP–TFBG. The error bars were determined from the spread of results from five measurements.

3.3. Analytical performance

The binding interaction and equilibrium information between the imprinted polymer and maltol template can be calculated from the Langmuir isotherm (Eq.1):

$$1/\Delta\lambda = 1/\Delta\lambda_{max} + 1/(\Delta\lambda_{max}KC) \qquad (1)$$

where $\Delta\lambda$ is the wavelength shift observed after binding of the maltol template to the polymer, and C is the concentration of the maltol solution. $\Delta\lambda_{max}$ represents the apparent maximum wavelength shift, and K is the Langmuir constant. The constants obtained from the linear form of the Langmuir isotherm by plotting $1/\Delta\lambda$ as a function of $1/C$ are $\Delta\lambda_{max} = 43.74$ pm and $K = 7\ 10^6\ M^{-1}$ respectively. The high value of the Langmuir constant (K) suggests that affinity of the binding sites is very strong.

The experimental calibration curve for $\Delta\lambda$ vs. C_{maltol} can be considered as linear up to 60 nM and then the slope (i.e. the sensitivity) decreases. The regression fit for the linear part is

$$\Delta\lambda = 6.3 \times 10^8 C_{maltol} + 5.4 (pm) \qquad (2)$$

With $R^2 = 0.9777$ and the limit of detection (LOD) is 8.1 nM or 1 ng/mL, calculated from the concentration that yields a signal which is 3 times the average noise level [45]. These experimental results show a good linearity for the sensor and a high sensitivity, 6.3×108 pm/M. The whole experimental processes were repeated twice and the samples were measured five times.

There is no comparative data for maltol sensors in the literature. However, a few studies using the molecular imprinting technique coupled with optical fibers can be used to evaluate our results. For instance, Cennamo et al. [47] realized an SPR-tapered plastic optical fiber for the detection of L-nicotine (MW=162 g/mol) and they determined a LOD of 1.86 10^{-4} M and a sensitivity of 1.3 10^7 pm/M, worse values than those obtained here. On the other hand, Verma and Gupta [46], using an SPR optical fiber for the detection of tetracycline (MW=481 g/mol), reported a huge sensitivity of 421 nm/μM (4.21 10^{11} pm/M), but the smallest measured concentration was only 20 nM, for a molecule four times heavier than ours. The spectral width of their resonance, i.e. ~ 170 nm (typical for conventional SPR), is 1.7×10^4 larger than ours, which explains that we could demonstrate a better LOD in spite of the lower sensitivity. The large difference in sensitivity however indicates that our maltol–MIP immobilized on the TFBG was likely not fully optimized and that its sensitivity could be improved further if necessary.

As maltol belongs to the low molecular weight molecules, it is possible to compare LODs obtained for similar molecules but using different kinds of transducers. For instance, Gultekin et al. reported a LOD of 7.8 nM for the detection of caffeic acid (MW=180 g/mol) using a MIP-based QCM nanosensor, Pietrzyk et al. [21] were able to detect 5 nM of histamine (MW=111 g/mol) using an acoustic sensor [47], while trinitrotoluene (MW=227 g/mol) was detected using an SPR sensor (in the standard Kretschmann configuration) with a LOD of 10 nM according to Bao et al. [48]. So while the LODs of these sensors are similar (nM level), the advantages of using a TFBG sensor come from the handling of the sensor. Indeed, all the sensors cited above are bulky, cumbersome instruments that are relatively expensive. On the other hand, with an optical fiber, the sensor head cost and dimension are reduced to minimal levels while remotely located, relatively inexpensive and smaller instrumentation developed for the telecommunication industry is readily available to interrogate the sensors. A further advantage of using TFBG devices is that they are inherently self-referenced for power levels and temperature. [18]

3.4. Determination of maltol content in complex samples

The maltol-imprinted polymer on TFBG was finally evaluated for the detection of maltol in a real food sample, a commercially available fruit jelly preparation (JELLO™). According to the package, this powder is composed of sugar, gelatin, adipic acid, fumaric acid, salt, artificial flavor, and color. The jelly powder was first diluted in water and tested just after reconstitution to avoid the jellification. Because no maltol is mentioned in the ingredients, samples were spiked with maltol solution at two concentrations, 10 nM and 50 nM. The same protocol of measurement used for the calibration curve was then followed. As the food sample is a complex medium made up of a number of constituents, a reference signature was first obtained by immersing the probe in the dissolved jelly solution without maltol. This reference spectrum shows a 20 ± 3 pm shift after rinsing and recording in water (relative to a sensor that was never exposed to jelly). It is clear that some molecules do not stick selectively to the probe surface. Most of the compounds in the food contain OH or COOH groups in their chemical structure, and therefore form hydrogen bonds easily. However, the size, shape and chemical functionalities of the ingredients are different from those of maltol and these molecules can only bind to the surface by non-specific interactions. In contrast, when the probe is immersed in a food sample spiked with maltol, bigger wavelength shifts are observed (Fig. 6). After subtracting the signal
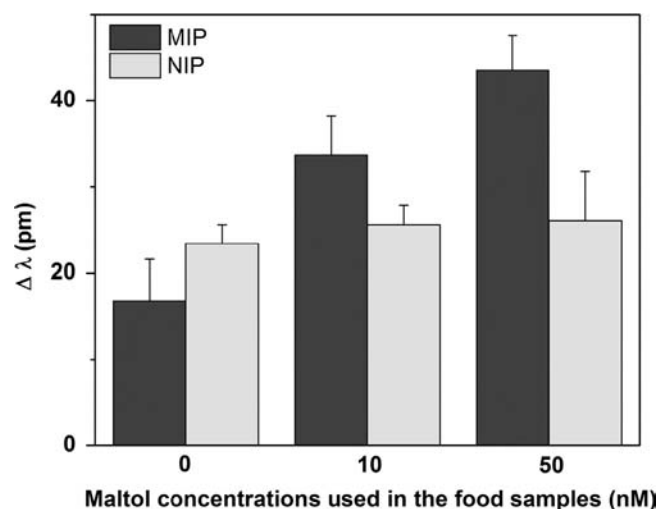

Fig. 6. Shifts obtained after immersing the maltol–MIP–TFBG (dark gray) and the NIP–TFBG (light gray) in a jelly powder diluted in water and then in spiked samples. The uncertainly limits were calculated using statistics from 5 measurements in each case.

Table 1
Detection of maltol in food samples.

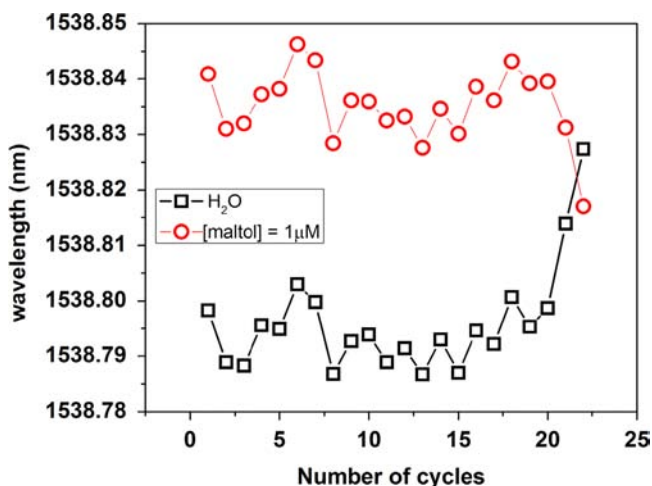|	Spiked concentration (mol L^{-1})	$\Delta\lambda$ (pm)	Measured concentration (mol L^{-1})	Recovery of maltol (%)
MIP	10 nM	16.9	8.8 nM	88
	50 nM	32.7	43.0 nM	86

Fig. 7. Stability of the maltol–MIP–TFBG. (For interpretation of the references to color in this figure, the reader is referred to the web version of this article.)

due to nonspecific binding, the concentrations of maltol in each sample were determined from the calibration curve using the $\Delta\lambda$ shift. For each sample, five measurements were performed and Table 1 summarizes the results.

The sensor response shows a detection level close to 87% of the actual maltol concentrations in a complex medium.

3.5. Sensor stability

As a final remark, it is interesting to report about the stability of the concentration measurement obtained by the Maltol–MIP–TFBG sensor after a large number of uses, with complete removal of the maltol from the MIP in between each experiment. Fig. 7 shows the starting wavelength of the sensor in pure water (black squares) prior to a maltol binding with the saturation concentration (red round). The average difference between the 2 measurements is 42.1 ± 0.06 pm until 20 cycles of use (i.e. one rebinding and measurement followed by one washing with methanol/acetic acid (80:20, v/v)). However, the difference drops at the 21st measurements which indicate a loss of the recognition. Some hypotheses can explain the phenomenon. Either the mirror at the downstream of the fiber is damaged or the molecular imprinted polymer lost its recognition capacity. In any event, for this study, the MIP–TFBG sensor designed could be used for up to 20 cycles without substantial degradation.

4. Conclusion

A nanocoated fiber sensor system based on a tilted fiber Bragg grating and a molecular imprinted layer has been presented and experimentally tested for the detection of maltol, a low molecular weight aroma enhancer. The probe was fabricated over an optical fiber using the molecular imprinting technique as a sensing layer. The experimental results indicate that the nanosensor exhibits good performance in terms of selectivity and sensitivity. The low limit of

detection (8.1 nM) ensures that the MIP–TFBG nanosensor can be used for the detection of aroma enhancers such as maltol in real food samples because these enhancers are usually only present in small quantities, due to their important aromatic power. The value of the Langmuir constant ($K = 7 \times 10^6$ M) shows that the affinity of the binding site for maltol molecules is strong. This sensor system is label-free and provides rapid measurements in real time. In addition to the fast response, the proposed MIP–TFBG sensor presents several advantages such as reusability, selectivity, low cost, easy handling and remote sensing. Since MIPs can be synthesized for many target analytes, a variety of selective MIP–TFBG sensors can be developed to extend their applications in many areas.

References

[1] M. Besler, Anal. Chem. 20 (2001) 662–672.
[2] A.J. Van Hengel, Anal. Bioanal. Chem. 389 (2007) 11–118.
[3] J. Pollet, F. Delport, K.P.F. Jansen, D.T. Tran, J. Wouters, T. Verbiest, J. Lammertyn, Talanta 83 (2011) 1436–1441.
[4] Y.-Q. Yang, X.-W. He, Y.-Z. Wang, W.-Y. Li, Y.-K. Zhang, Biosens. Bioelectron. 54 (2014) 266–272.
[5] S.P. Wren, T.H. Nguyen, P. Gascoine, R. Lacey, T. Sun, K.T.V. Grattan, Sens. Actuators B-Chem. 193 (2014) 35–41.
[6] S.Z. Bajwa, R. Dumler, P.A. Lieberzeit, Sens. Actuators B-Chem. 192 (2014) 522–528.
[7] W. Cheng, H. Ma, L. Zhang, Y. Wang, Talanta 120 (2014) 255–261.
[8] K. Haupt, Anal. Chem. 75 (2003) 376A–383A.
[9] S. Li, X. Huang, M. Zheng, W. Li, K. Tong, Sensors 8 (2008) 2854–2864.
[10] B.B. Prasad, D. Jauhari, M.P. Tiwari, Biosens. Bioelectron. 50 (2013) 19–27.
[11] T.-P. Huynh, P. Pieta, F. D'Souza, W. Kutner, Anal. Chem. 85 (2013) 8304–8312.
[12] S. Tian, Z. Guo, X. Zhang, X. Wu, Anal. Methods 5 (2013) 5179–5187.
[13] R. Schirhagl, U. Latif, D. Podlipna, H. Blumenstock, F.L. Dickert, Anal. Chem. 84 (2012) 3908–3913.
[14] T. Guo, F. Liu, Y. Liu, N.-K. Chen, B.-O. Guan, J. Albert, Biosens. Bioelectron. 55 (2014) 452–458.
[15] G. Tsigaridas, D. Polyzos, A. Ioannou, M. Fakis, P. Persephonis, Sens. Actuators A-Phys. 209 (2014) 9–15.
[16] H.-T. Sun, E.-C. Chang, H.-J. Sheng, C.-C. Chen, W.-F. Liu, Microw. Opt. Technol. Lett. 54 (2012) 681–684.
[17] N. Cennamo, G. D'Agostino, M. Pesavento, L. Zeni, Sens. Actuators B-Chem. 191 (2014) 529–536.
[18] J. Albert, L.-Y. Shao, C. Caucheteur, Laser Photonics Rev. 7 (2012) 1–26.
[19] M. Pesavento, G. D'Agostino, G. Alberti, R. Biesuz, D. Merli, Anal. Bioanal. Chem. 405 (2013) 3559–3570.
[20] M.C. Blanco-López, M.J. Lobo-Catañón, A.J. Miranda-Ordieres, P. Tuñón-Blanco, TrAC Trends Anal. Chem. 23 (2004) 36–48.
[21] A. Gultekin, G. Karanfil, M. Kus, S. Sonmezoglu, R. Say, Talanta 119 (2014) 533–537.
[22] K. Kantarovich, I. Tsarfati-BarAd, L.A. Gheber, K. Haupt, I. Bar, Plasmonics (2013) 3–12.
[23] Z. Altintas, Y. Uludag, Y. Gurbuz, I. Tothill, Anal. Chim. Acta 712 (2012) 138–144.
[24] H. Bao, T. Wei, H. Meng, B. Liu, Chem. Lett. 41 (2012) 237–239.
[25] S.K. Srivastava, R. Verma, B.D. Gupta, Sens. Actuators B-Chem 153 (2011) 194–198.
[26] A. Bialiayeu, A. Bottomley, D. Prezgot, A. Ianoul, J. Albert, Nanotechnology 23 (2012) 44412.
[27] S. Lepinay, A. Staff, A. Ianoul, J. Albert, Biosens. Bioelectron. 52 (2014) 337–344.
[28] Y. Shevchenko, T.J. Francis, D.A.D. Blair, R. Walsh, M.C. Derosa, J. Albert, Anal. Chem. 83 (2011) 7027–7034.
[29] V. Voisin, J. Pilate, P. Damman, P. Mégret, C. Caucheteur, Biosens. Bioelectron. 51 (2014) 249–254.
[30] S. Maguis, G. Laffont, P. Ferdinand, B. Carbonnier, K. Kham, T. Mekhalif, M.C. Millot, Opt. Express 16 (2008) 19049–19062.
[31] L.R. Bernstein, T. Tanner, C. Godfrey, B. Noll, Metal-Based Drugs 7 (2000) 33–47.
[32] N. Kaneko, H. Yasui, J. Takada, K. Suzuki, H. Sakurai, J. Inorg. Biochem. 98 (2004) 2022–2031.
[33] B.D. Liboiron, K.H. Thompson, G.R. Hanson, E. Lam, N. Aebischer, C. Orvig, J. Am. Chem. Soc. 127 (2005) 5104–5115.
[34] D.M. Reffitt, T.J. Burden, P.T. Seed, J. Wood, R.P.H. Thompson, J.J. Powell, Ann. Clin. Biochem. 37 (2000) 457–466.
[35] J. Thamm, Food Additives: What Are You Putting in Your Mouth? 2001.
[36] UE European commission flavouring substances 2013.

[37] H.-B. Zhu, Y.-C. Fan, Y.-L. Qian, H.-F. Tang, Z. Ruan, D.-H. Liu, H. Wang, Chin. Chem. Lett. (2014), http://dx.doi.org/10.1016/j.cclet.2013.12.001.

[38] Corning 2010, Corning SMF-28 ULL Optical fiber with corning ultra low-loss technology. ⟨http://www.corning.com/opticalfiber/products/SMF-28_ULL_fiber.aspx⟩ (accessed on 17.03 2014).

[39] C.-F. Fan, C. Chen, A. Jafari, A. Laronche, D.J. Thomson, J. Albert, Appl. Opt. 46 (2007) 1142–1149.

[40] S. Hrapovic, Y.L. Liu, G. Enright, F. Bensebaa, J.H.T. Luong, Langmuir 9 (2003) 3958–3965.

[41] R.L. Kass, J.L. Kardos, Polym. Eng. Sci. 1 (1971) 11–18.

[42] A. Lagha, N. Adhoum, L. Monser, Open Chem. Biomed. Methods J. 4 (2011) 7–13.

[43] S.A. Mohajeri, G. Karimi, J. Aghamo-hammadian, M.R. Khansari, J. Appl. Polym. Sci. 121 (2011) 3590–3595.

[44] R.E. Kartasasmita, A.N. Hasanah, S. Ibrahim, J. Chem. Pharm. Res. 5 (2013) 351–355.

[45] J. Vial, A. Jardy, Anal. Chem. 71 (1999) 2672–2677.

[46] R. Verma, B.D. Gupta, Analyst 138 (2013) 7254–7263.

[47] A. Pietrzyk, S. Suriyanarayanan, W. Kutner, R. Chitta, F. D'Souza, Anal. Chem. 82 (2009) 2633–2643.

[48] H. Bao, T.X. Wei, X.L. Li, Z. Zhao, H. Cui, P. Zhang, Chin. Sci. Bull. 57 (2012) 2102–2105.